Signal detection efficiency in multiphoton ionization flame measurements

Kermit C. Smyth and Paul J. H. Tjossem

Multiphoton ionization is often the most sensitive method available for detecting radical species in flame environments. To make accurate relative concentration measurements, however, the electron (or ion) detection efficiency as a function of flame position must be known. Two methods are presented for determining this quantity in a laminar CH_4/air diffusion flame burning at atmospheric pressure: (1) simultaneous detection of ionization and fluorescence in CO, following two-photon excitation of the $B^1\Sigma^+$ state at 230.0 nm; (2) comparison of 3 + 1 multiphoton ionization of the $4s'$ state of argon at 314.4 nm with mass spectrometric measurements. The results show significant variation of the electron detection efficiency in the lean, stoichiometric, and rich flame regions, with the greatest detection sensitivity observed in the high-temperature, primary reaction zones (i.e., near stoichiometric conditions). Corrections to multiphoton ionization data obtained for H atoms are discussed in terms of determining relative concentration profiles across the methane/air diffusion flame.

I. Introduction

Resonance-enhanced multiphoton ionization (MPI) has been successfully applied to the detection of numerous free radicals and stable species in flames, including H atom,[1–6] O atom,[3,4,7] C atom,[8,9] CH·,[9] CO,[5,10] O_2,[9] NO·,[11,12] PO·,[13] CH_3·,[8,14,15] HCO·,[15,16] C_2O,[5] and *trans*-1,3-butadiene.[17] Multiphoton ionization methods exhibit high sensitivity and are the only practical optical approach for monitoring minor species when fluorescence quantum yields are low, such as for the methyl (CH_3·) radical. Low fluorescence quantum yields are also expected for larger hydrocarbon radicals of combustion interest, such as ethynyl (C_2H·), vinyl (C_2H_3·), and phenyl (C_6H_5·). Active investigation to find suitable electronic transitions for MPI detection of these species is currently underway, since they are presently observable only in environments where molecular beam mass spectrometric sampling can be utilized, for example, in low pressure premixed flames.

In flame studies it is desirable to measure accurate absolute and relative concentration profiles for the reactive radical species. Multiphoton ionization approaches using sharply focussed laser beams and localized electron collection offer excellent spatial resolution. However, when using MPI methods, it is also necessary to establish how well the laser-produced electrons are detected as a function of flame position. The electron detection efficiency will vary whenever the local electric field changes, for instance, when the local ion density varies with flame position. The same concern arises when making MPI profile measurements in plasmas, in diamond film and chemical vapor deposition experiments, and in high temperature materials processing investigations.

This paper presents two methods by which the relative electron detection efficiency can be determined for the analysis of MPI profile data on H atoms obtained in a CH_4/air diffusion flame at atmospheric pressure.[6] In the first case the MPI and laser-induced fluorescence (LIF) signals from the $B^1\Sigma^+$ state of CO are simultaneously measured, while the second method compares the multiphoton ionization signal arising from argon atoms with a separate mass spectrometric measurement. Ideally, one would like to determine the relative electron detection efficiency using a single species which occurs naturally in all flame regions. Our experiments on CO give useful results in the rich and stoichiometric zones, while those on argon are complementary, providing data in the lean and stoichiometric regions. Since the CO MPI and LIF data are obtained simultaneously and with laser conditions close to those of our earlier H-atom measurements,[6]

When this work was done, both authors were with U.S. National Institute of Standards & Technology, Center for Fire Research, Gaithersburg, Maryland 20899; Paul Tjossem is now with Grinnell College, Physics Department, Grinnell, Iowa 50112.

Received 5 January 1990.

this method is preferred for analyzing the H-atom profiles.

II. Experimental Approach

The H-atom multiphoton ionization profile data have been obtained using low laser intensities and a Doppler-free configuration to avoid the photolytic production of H atoms.[6] Figure 1 shows the burner and optical arrangement for these experiments. An overventilated, laminar methane (99.9% purity)/air diffusion flame was stabilized on a Wolfhard-Parker slot burner at atmospheric pressure; fuel flows from the central slot (width = 8 mm) and air from each of the two outside slots (width = 16 mm). This burner produces a flame with two identical, 2-D flame sheets, which greatly facilitates making precise lateral profile measurements (in the x-direction in Fig. 1). Flame conditions were the same as those used previously when the profiles of chemical species concentrations,[6,8,18–20] temperature,[18] and velocity[18] were determined. Measurements to deduce the electron detection efficiency as a function of the lateral position are reported here for a height of 9 mm above the burner, where profile data on OH·,[20] H atoms,[6] and O atoms[6] have been obtained. This is a convenient region for the analysis of the flame chemistry,[21,22] since hydrocarbon concentrations are appreciable but significant amounts of soot have not yet formed.[18]

The CH_4/air diffusion flame exhibits steep temperature and concentration gradients,[18] and at 9 mm above the burner the local equivalence ratio varies from 0.2 in the lean regions (at ±10 mm from the burner centerline) to 50 in the rich region at the burner centerline. The local ion density is expected to vary strongly as a function of flame position,[23] with maximum concentrations of $\approx 10^{11}$ ions/cm^3 appearing near the high temperature reaction zones.[24] These primary reaction zones are more conducting than the cooler rich and lean regions. Multiphoton ionization measurements have often been made by inserting a single tungsten electrode into this flame, biased at either positive or negative voltage with the burner grounded.[8] Since the local ion density and the local ion production rate vary with flame position, the local electric field and the electron detection efficiency will also change.

The dual electrode configuration shown in Fig. 1 has been adopted to minimize the influence of the grounded burner upon the measurement of laser-induced ionization signals. Two 0.56-mm diam tungsten rods are spaced 0.5 mm apart, with one rod biased at +600 V and the second rod and the burner grounded. This arrangement creates a high electric field near the rods. Directing the electrodes perpendicular to the burner axis and the laser beam direction has several advantages: flame perturbations are minimized; the electron signal is detected in a localized region; and the observed profiles are symmetric (in other electrode geometries small deviations from two-dimensionality of the flame sheets can give rise to asymmetric profile shapes). However, profile measurements cannot be made in this flame geometry by directing the laser beam into the region of highest field (and therefore largest laser-induced signal[25]) between the electrodes. Rather, the laser beam is typically positioned just below the two electrodes (within 1 mm).

The multiphoton ionization measurements on H at-

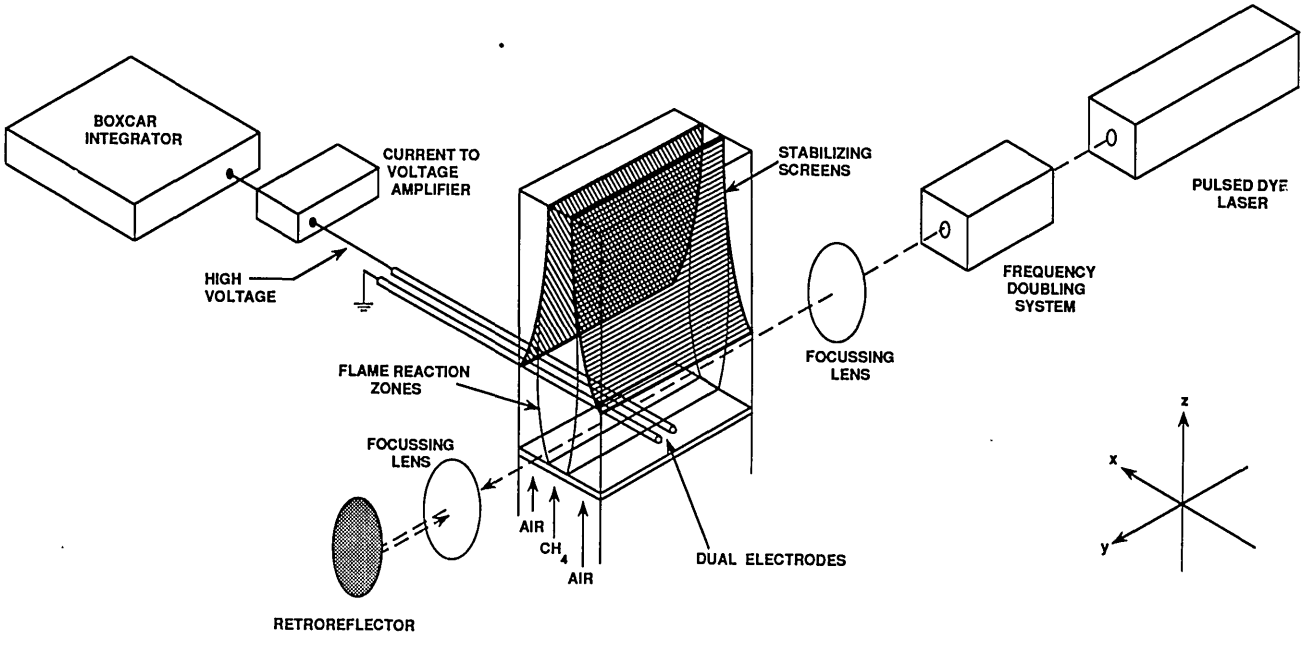

Fig. 1. Schematic diagram of the Wolfhard-Parker slot burner (central fuel slot is 8 mm wide and 41 mm long; air slots are 16 mm wide and 41 mm long[18]) and the optical setup for making Doppler-free multiphoton ionization measurements using a dual electrode arrangement. Laser-induced fluorescence was detected at 90° to the direction of the laser beams.

oms involved the two-photon excitation of the 1s →→ 2s transition at 243 nm, followed by absorption of a third photon which leads to ionization (a 2 + 1 ionization process). Since the electron detection efficiency is sensitive to the local electric field, experimental conditions have been used which match as closely as possible those of the H-atom study.[6] Variables which are easy to control and reproduce include the electrode configuration, the applied potential, the detection electronics, and the flame location (height above burner and lateral position). The detection sensitivity can also depend upon the size of the observed signal.[4] If the laser-induced ion density is greater than that which occurs naturally in the flame, then the local steady state electric field distribution will undergo a transient perturbation during the laser pulse.[25] In addition, electron-ion recombination rates will vary with the local ion density.[26] The signal level is a variable which can be controlled only roughly, since it depends upon the local concentration of the species being ionized, the photon intensity, and the number of photons required in the rate-limiting excitation step of the multiphoton ionization process.

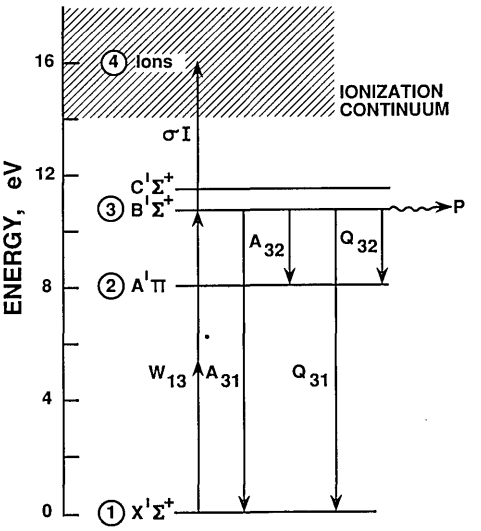

Fig. 2. Energy level diagram of the electronic states of CO; W_{13}, A, σI, P, and Q represent the rates of two-photon absorption, radiative decay, ionization, predissociation, and total quenching, respectively.

A. CO Measurements

The $B^1\Sigma^+$ state of CO can be readily excited by the absorption of two phtons at 230.0 nm,[10] and both ionization (a 2 + 1 process) and fluorescence from this electronic state can be detected. Figure 2 presents the relevant energy levels of CO. Using the notation of this figure, the rate of change of the $B^1\Sigma^+$ state population can be written as

$$dN_3/dt = N_1W_{13} - N_3(Q + A + P + \sigma I), \quad (1)$$

where W_{13} is the rate coefficient for two-photon absorption, Q is the total quenching rate, A is the radiative rate, P is the predissociation rate, and σI is the ionization rate. The radiative lifetime of the $B^1\Sigma^+$ state is 21.8 ns,[27] which gives a value for A much smaller than Q and σI for our experimental conditions.[10] In addition, $P = 0$ for the low rotational levels at the Q-branch head for the $v' = 0$ vibrational state.[10] Therefore, if one excites the CO $B^1\Sigma^+ \leftarrow X^1\Sigma^+$ (0,0) band at the Q-branch head using laser intensities far from saturation, the observed $B^1\Sigma^+ \rightarrow A^1\Pi$ fluorescence and ionization (MPI) signals are proportional to their branching ratios multiplied by their respective detection efficiencies:

$$\text{MPI signal} \propto N_3 \cdot [\sigma I/(Q + \sigma I)] \cdot M(x), \quad (2)$$

$$\text{LIF signal} \propto N_3 \cdot [A/(Q + \sigma I)] \cdot F(x). \quad (3)$$

Here the total loss rate $(Q + A + P + \sigma I)$ has been simplified: Q and σI are much greater than A and P in Eq. (1). $M(x)$ is the relative electron detection efficiency as a function of flame position, and $F(x)$ is the corresponding relative photon detection efficiency. Since the flame is optically thin, $F(x) = 1$ for a fixed collection geometry. Therefore, the ratio of the multiphoton ionization and the fluorescence signals yields the relative electron detection efficiency directly,

$$\text{MPI signal/LIF signal} = M(x) \cdot \text{constant}. \quad (4)$$

For a given laser intensity, $M(x)$ can be measured independently of the local CO concentration and the quenching rate Q.

The CO measurements were carried out under the same optical experimental conditions as those described recently.[10] The output beam from a nitrogen pumped dye laser (400–500 μJ/pulse, 7-ns duration) was focussed into a beta-barium borate (BBO) crystal, which was mounted in an autotracker to produce tunable, linearly polarized radiation at 230 nm with energies up to 100 μJ/pulse. A 100-mm f.l. lens was used to focus the laser beam, as was also the case for the H-atom experiments.[6] The Q-branch head of the (0,0) band in the $B^1\Sigma^+$ state was excited by the absorption of two photons at this wavelength, and both the 2 + 1 multiphoton ionization signal and the $B^1\Sigma^+ \rightarrow A^1\Pi$ laser-induced fluorescence signal were monitored simultaneously. The MPI electron signal was detected with the dual electrode arrangement shown in Fig. 1, amplified with a current-to-voltage amplifier (Analog model 50K[28]) and then processed with a boxcar averager whose ≈ 1-μs gate monitored the central half of the amplified signal. Laser-induced fluorescence at 483.5 nm from the (0,1) band of the $B^1\Sigma^+ \rightarrow A^1\Pi$ transition was observed perpendicular to the laser beam direction using a dielectric filter (FWHM = 10 nm centered at 480 ± 2 nm) and photomultiplier tube combination.

The polarization ratio (signal with linear polarization divided by that observed with circular polariza-

tion) has been found to exceed 300 for the $B^1\Sigma^+ \leftarrow X^1\Sigma^+$ transition of CO at the (0,0) Q-branch head.[10] Simply by changing the polarization of the incoming laser beam at constant intensity, the excitation rate of the B state can be varied by this sizable factor. A large observed polarization ratio (checked using a UV-quartz Babinet-Soleil compensator) ensures that the MPI and fluorescence signal detection is not perturbed by space charge effects or photomultiplier tube gain saturation, respectively, at the highest signal levels. On the other hand, a small measured polarization ratio is an indication that the largest signals are not being detected accurately.

No change in the CO fluorescence profile was observed when the dual electrode was removed from the flame. The SNR for the multiphoton ionization measurements was typically at least ten times higher than for the laser-induced fluorescence data (see Fig. 4 in Sec. III).

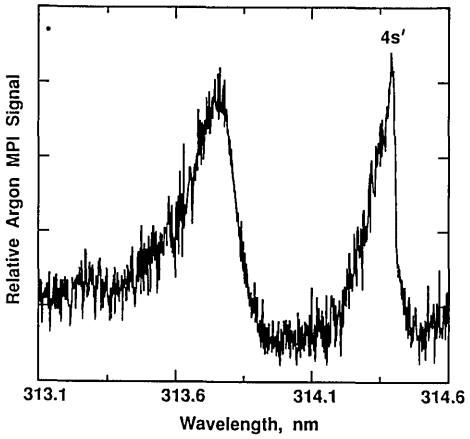

Fig. 3. Multiphoton ionization spectrum in the region of the argon $3p^6\ ^1S \rightarrow\rightarrow\rightarrow 3p^5 4s\ 4s'[1/2]^\circ\ J = 1$ transition at 314.4 nm (a 3 + 1 process), obtained with an additional 1% argon added to air at room temperature. The zero signal level is at the origin.

B. Argon Measurements

The second method of determining the electron detection efficiency as a function of flame position involves comparing the MPI signals from the $4s'$ state of argon with mass spectrometric profile data obtained by means of quartz microprobe sampling.[18] In air the argon concentration is approximately 1%, and its mole fraction is constant as a function of flame position in the oxidizer flows (see Fig. 1) to a lateral position of ± 4.2 mm at a height of 9 mm above the burner[29] (the slot separators between the fuel and oxidizer flows are located at ± 4.0 mm, and the buoyant diffusion flame entrains air[18]). An additional 1% argon was added to the air flows to improve the argon MPI signals relative to hydrocarbon ionization in rich flame regions (see Sec. III).

Observation of the 3 + 1 multiphoton ionization signal for the argon $3p^6\ ^1S \rightarrow\rightarrow\rightarrow 3p^5 4s\ 4s'[1/2]^\circ\ J = 1$ transition at 314.4 nm requires a retroreflected beam geometry to avoid near complete cancellation of the MPI signal by third harmonic generation.[30] A Nd:YAG pumped tunable dye laser was frequency doubled to produce 0.55 mJ, 7-ns pulses, and two 100 mm f.l. lenses were used. The MPI spectrum of argon exhibits complex pressure-dependent structure at wave-lengths shorter than the $4s'$ resonance at 314.4 nm.[30] However, the intensity of the $4s'$ signal itself has been found to be relatively linear with pressure.[30] Figure 3 shows the argon MPI spectrum measured for a 2% argon concentration in air at room temperature. Profile measurements have been made by tuning the laser wavelength to the peak of the $4s'$ resonance. Subsequent analysis is based upon the assumption that the magnitude of the argon MPI signal depends only on the argon number density.

III. Results

All of the multiphoton ionization profile measurements were made under conditions identical to those used in the H-atom experiments[6]: the dual electrode was oriented perpendicular to the laser beam direction and centered along the y-direction (see Fig. 1), one electrode was biased at +600 V, and the laser beam was positioned at a height of 9 mm above the burner and just below (within 1 mm) the two electrodes. In addition, the first focussing lens was translated along the beam direction to obtain the maximum MPI signal. Profile data were taken with the laser wavelength tuned to the CO and argon resonances of interest and also tuned off resonance. In the rich regions of the CH_4/air diffusion flame there exist numerous hydrocarbon species,[18] which can readily ionize by absorbing two ultraviolet photons (1 + 1 multiphoton ionization of polyenes, polyynes, and polycyclic aromatic compounds). This interfering ionization signal is nonresonant and can be removed by simply subtracting the off-resonance profile from the on-resonance profile.

Figure 4 presents the CO results obtained using multiphoton ionization and laser-induced fluorescence. The fluorescence profiles also show non-resonant background interference in the rich flame regions, which appears as emission at 480 nm excited at 230 nm. This laser-induced fluorescence is broadband and has also been attributed to polycyclic aromatic hydrocarbons, as well as possibly to polyenes and polyynes.[18,31,32]

Even in the original data of Fig. 4 it is apparent that the MPI and LIF profiles for CO are different; the MPI data show distinct peaks at a lateral position of ± 5.6 mm and a much weaker signal at the burner centerline. The net (subtracted) MPI and LIF profiles are also recorded in Fig. 4. To determine the relative electron detection efficiency, the net MPI profile is divided by the LIF data. This procedure is reliable from the burner centerline out to a lateral position of ± 6.0 mm. At greater lateral distances both the MPI and LIF signals fall sharply, and their ratio is not reproducible.

Observation of a large polarization ratio at the Q-branch head ensured that the electron signal collection was not space charge limited[10]; at lower laser intensity the shape of the MPI profile was the same. Experi-

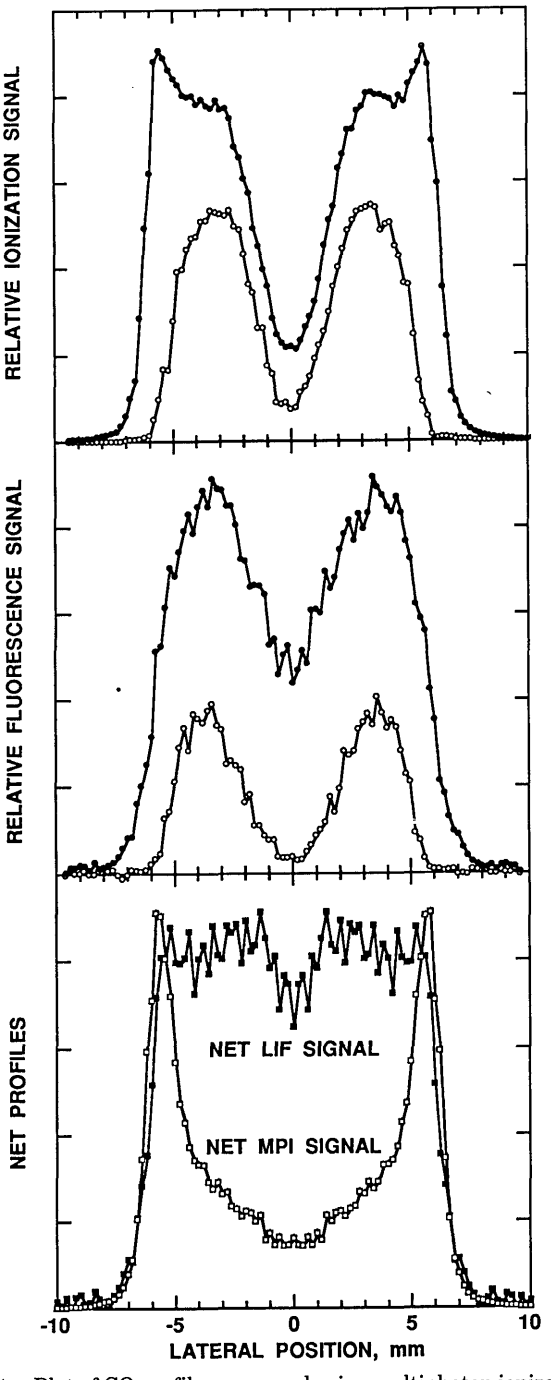

Fig. 4. Plot of CO profiles measured using multiphoton ionization (upper panel) and laser-induced fluorescence (middle panel) at a height of 9 mm above the burner; the original data are shown with the laser wavelength tuned on resonance (solid symbols; laser wavelength is 230.0 nm) and off resonance (open symbols). Bottom panel: net (subtracted) profiles; the MPI (□) and LIF (■) data have been symmetrized (centered and the two sides averaged). The zero signal levels are at the origin for each panel.

ments were also carried out with a bias of +300 V on the anode to check for possible signal amplification effects; again the MPI profile was unchanged. However, the shape of the CO MPI profile was found to be sensitive to the position of the laser beam focus. In

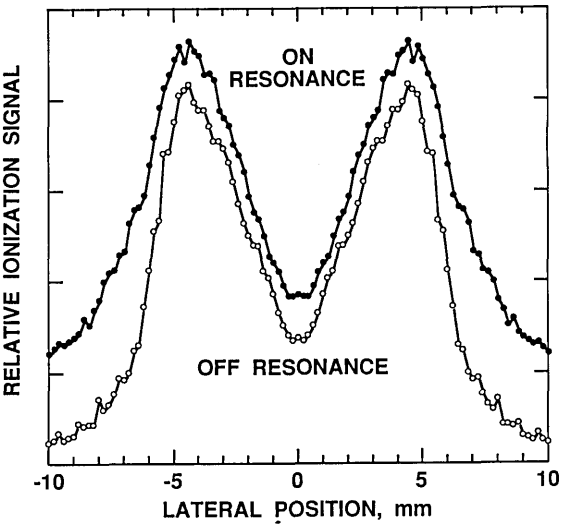

Fig. 5. Argon profiles measured using multiphoton ionization at a height of 9 mm above the burner; the original data have been symmetrized and are shown with the laser wavelength tuned on resonance (solid symbols ●; 314.4 nm) and off resonance (open symbols ○). The zero signal level is at the origin.

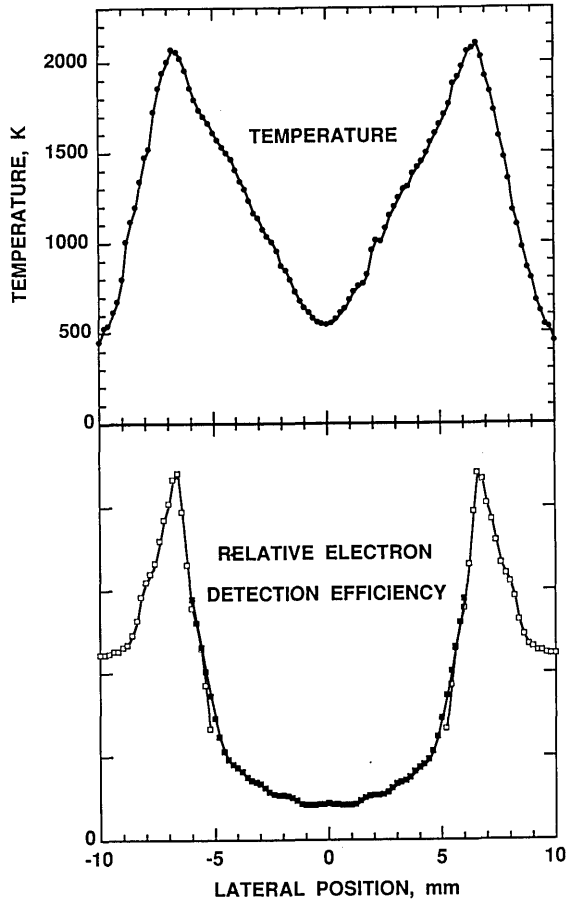

Fig. 6. Lower panel: the relative electron detection efficiency determined at height of 9 mm above the burner; the solid symbols (■) are derived from the CO data and the open symbols (□) are from the argon results. The zero signal level is at the origin. Upper panel: radiation-corrected thermocouple temperature measurements[18] at the same height.

particular, translation of the laser spot 2.0 mm toward the anode gave a profile with reduced signal levels and without the peaks at ± 5.6 mm, i.e., a shape closer to that of the LIF profile. These experimental conditions did not replicate those of the H-atom measurements, and so the results were not used to derive an electron detection efficiency for analysis of the H-atom data.

Figure 5 presents the original data for the argon multiphoton ionization profiles, again obtained with the laser wavelength tuned on and off resonance. In this case, the interfering hydrocarbon ionization in rich flame regions overwhelms the small argon MPI signal. The argon MPI data are useful in the region from ±10.0 to ±5.2 mm. Since the argon mole fraction is constant here, the net argon MPI signals can be used directly to derive the electron detection efficiency. The results for CO and argon overlap in the limited region from ±5.2 to ±6.0 mm, where the agreement between the two data sets is excellent. The CO and argon measurements are linked together at ±5.8 mm; the original net profile data were smoothed three times with a Savitzky-Golay filter[33] in the analysis. Figure 6 presents the derived relative electron detection efficiency at 9 mm above the burner and the measured temperature profile.[18]

IV. Discussion

The most striking result of the present investigation is the large variation in electron detection efficiency measured as a function of flame position (Fig. 6). This is perhaps not surprising in view of the steep temperature and concentration gradients which occur in an atmospheric-pressure diffusion flame.[18] In essence, the CH_4/air flame presents a position-dependent matrix effect for the detection of electrons in a multiphoton ionization experiment.[25] The collected signal depends upon the local electric field and upon the position of laser-induced electron production. Where ionization levels and ion generation rates are high, the local electric field gradient will be large for a given electrode geometry and applied bias voltage.[25] The flame regions of highest conductivity, therefore, will exhibit the largest electron detection efficiency and signal levels. One expects that this will occur close to the high temperature, primary reaction zones, where maximum ion concentrations have been detected[24] and ion production rates due to the chemi-ionization process[23]

$$CH\cdot + O{:} \rightarrow CHO^+ + e^- \qquad (5)$$

will be greatest. Figure 6 shows that the peak flame temperatures and the highest electron detection efficiency do coincide.

Figure 7 presents our original H-atom multiphoton ionization data and the H-atom profile corrected for the variation in electron detection efficiency versus lateral flame position. The observed MPI profile for H atoms is narrow (FWHM = 0.9 mm), with signals detected over the region ± 5.0 to ± 8.2 mm. Here the electron detection efficiency does vary significantly;

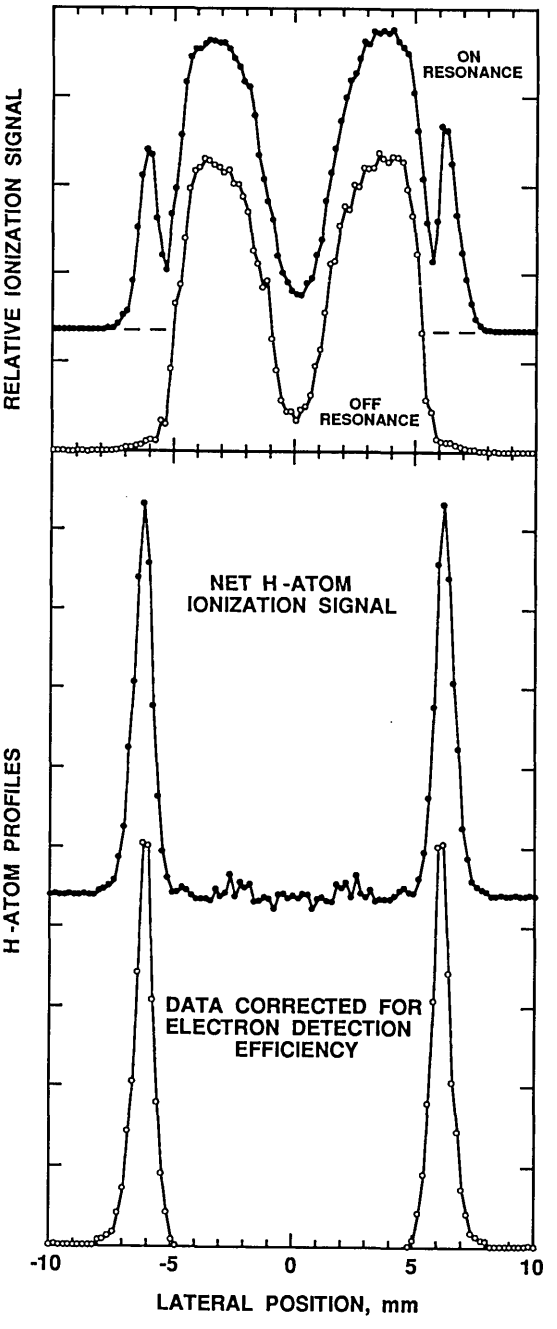

Fig. 7. Upper panel: H-atom profiles measured by Doppler-free multiphoton ionization (a 2 + 1 process at 243 nm[6]) at a height of 9 mm above the burner; the original data are shown with the laser wavelength tuned on (●) and off (○) resonance. The curves are offset for clarity, and the dashed line indicates the zero signal level for the on-resonance data. Lower panel (expanded vertical scale): net H-atom profile (●), the subtracted data have been symmetrized, and the H-atom profile corrected for the variation of the electron detection efficiency with flame position (○). The corrected data are presented only over the region where the H-atom measurements are reliable, ± 5.0–10.0 mm (see text). The zero signal levels occur in the lean flame regions (± 8–10 mm).

the resulting H-atom profile is shifted slightly toward rich flame regions and its shape is altered. These changes are small, but they are important for the analysis of chemical production rates in this CH_4/air diffusion flame. For a species which exhibits a broader concentration profile near the high temperature reaction zones, the correction to the MPI data would be greater (for example, see the CO data in Fig. 4).

There are relatively few additional candidate species which might be utilized for determining the relative electron detection efficiency over wide spatial regions of a flame. For better characterized flame systems, more options become available. The most direct measurements are those in which multiphoton ionization and laser-induced fluorescence signals can be observed simultaneously, as carried out for CO in this study. NO· is another possibility for such measurements. Fluorescence from NO· has been detected in premixed CH_4/air flames at atmospheric pressure.[34] The one-photon excitation of the $A^2\Sigma^+$ state of NO· is much more efficient than the two-photon absorption required for the excitation of the $B^1\Sigma^+$ state in CO. However, the radiative lifetime is much longer for NO· (200 ns[35] vs 21.8 ns[27]), the naturally occurring NO· concentration is much lower than that of CO (<0.1% vs 3–4%[29]), and NO· has an open rotational structure for the $A^2\Sigma^+ \leftarrow X^2\Pi_i$ transition[11] compared to the compact CO Q-branch.[10]

A second possible candidate for measuring the electron detection efficiency is N_2, where our mass spectrometric profile data[18] corrected for CO and C_2H_4 contributions could be compared with 3 + 1 multiphoton ionization results.[36] Excitation of a given rotational level would yield a profile from which the total N_2 relative concentration could be determined knowing the local temperature.[18] Comparison of ionization and fluorescence signals from H atoms and O atoms could also be utilized in special circumstances. For H atoms the two-photon excitation of the $n = 3$ levels would allow observation of emission at 656 nm (the $n = 3 \rightarrow n = 2$ Balmer transition). Careful attention to avoid the photolytic production of H atoms would be required in hydrocarbon flames.[6,37,38] The fluorescing $3p^3P$ state of O atom can be detected following two-photon excitation at 226 nm. However, the 2 + 1 ionization signal is typically overwhelmed by the 1 + 1 ionization from the NO· $A^2\Sigma^+$—$X^2\Pi_i$ (0,0) band in flames containing nitrogen.

The measurements reported here deserve a final word of caution: the relative electron detection efficiency shown in Fig. 5 has been found to be sensitive to the location of the laser beam focus relative to the electrodes. This variable is clearly not easy to reproduce in making successive measurements at different wavelengths with different dye lasers on H atoms (243 nm), CO (230 nm), and argon (314 nm). It may also be important to use a wider detection gate to integrate the entire electron and positive ion signals at the cost of reduced signal-to-noise levels,[25] since the different mobilities of H^+ and CO^+ may introduce different positive ion contributions to the observed signal.[39]

V. Conclusions

The efficiency of detecting electrons in multiphoton ionization experiments is found to vary significantly with spatial location in a CH_4/air diffusion flame burning at atmospheric pressure. For typical operating conditions with a dual-electrode configuration, the maximum detection efficiency occurs in the high-temperature, primary reaction zones. This result is attributed to variations in the local electric field as a function of flame position. Profile measurements obtained using multiphoton ionization methods can show significant changes when the data are corrected for the relative electron detection efficiency.

The results from this study show that it is important to measure the relative electron detection efficiency when attempting to deduce concentration profile information from multiphoton ionization data. This will be necessary for any environment wherein the local electric field is not uniform as a function of position.

We thank J. Houston Miller (George Washington University), John Miller (Oak Ridge National Laboratory), and John C. Travis (NIST) for many stimulating discussions concerning profile measurements, argon multiphoton ionization experiments, and electron detection in flames. We appreciate the expert assistance of Nelson P. Bryner in the preparation of the figures.

References

1. J. E. M. Goldsmith, "Resonant Multiphoton Optogalvanic Detection of Atomic Hydrogen in Flames," Opt. Lett. **7**, 437–439 (1982).
2. P. J. H. Tjossem and T. A. Cool, "Detection of Atomic Hydrogen in Flames by Resonance Four-Photon Ionization at 365 nm," Chem. Phys. Lett. **100**, 479–483 (1983).
3. J. E. M. Goldsmith, "Flame Studies of Atomic Hydrogen and Oxygen Using Resonant Multiphoton Optogalvanic Spectroscopy," in *Twentieth Symposium (International) on Combustion* (Combustion Institute, Pittsburgh, PA, 1984), p. 1331.
4. J. E. M. Goldsmith, "A Comparison of Resonant Multiphoton Optogalvanic and Fluorescence Detection for Combustion Diagnostics," presented at the Fall Meeting of the Western States Section of the Combustion Institute, Paper 62 (1984).
5. P. J. H. Tjossem and T. A. Cool, "Species Density Measurements with the REMPI Method; the Detection of CO and C_2O in a Methane/Oxygen Flame," in *Twentieth Symposium (International) on Combustion* (Combustion Institute, Pittsburgh, PA, 1984), p. 1321.
6. K. C. Smyth and P. J. H. Tjossem, "Relative H-Atom and O-Atom Concentration Measurements in a Laminar, Methane/Air Diffusion Flame," *Twenty-Third Symposium (International) on Combustion* (Combustion Institute, Pittsburgh, PA, 1990), in press.
7. J. E. M. Goldsmith, "Resonant Multiphoton Optogalvanic Detection of Atomic Oxygen in Flames," J. Chem. Phys. **78**, 1610–1611 (1983).
8. K. C. Smyth and P. H. Taylor, "Detection of the Methyl Radical in a Methane/Air Diffusion Flame by Multiphoton Ionization Spectroscopy," Chem. Phys. Lett. **122**, 518–522 (1985).
9. P. J. H. Tjossem and K. C. Smyth, "Multiphoton Ionization Detection of CH, Carbon Atoms, and O_2 in Premixed Hydrocarbon Flames," Chem. Phys. Lett. **144**, 51–57 (1988).

10. P. J. H. Tjossem and K. C. Smyth, "Multiphoton Excitation Spectroscopy of the $B^1\Sigma^+$ and $C^1\Sigma^+$ Rydberg States of CO," J. Chem. Phys. **91,** 2041–2048 (1989).
11. W. G. Mallard, J. H. Miller, and K. C. Smyth, "Resonantly Enhanced Two-Photon Photoionization of NO in an Atmospheric Flame," J. Chem. Phys. **76,** 3483–3492 (1982).
12. B. H. Rockney, T. A. Cool, and E. R. Grant, "Detection of Nascent NO in a Methane/Air Flame by Multiphoton Ionization," Chem. Phys. Lett. **87,** 141–144 (1982).
13. K. C. Smyth and W. G. Mallard, "Two-Photon Ionization Processes of PO in a C_2H_2/Air Flame," J. Chem. Phys. **77,** 1779–1787 (1982).
14. U. Meier and K. Kohse-Höinghaus, "REMPI Detection of CH_3 in Low-Pressure Flames," Chem. Phys. Lett. **142,** 498–502 (1987).
15. T. A. Cool, J. S. Bernstein, X.-M. Song, and P. M. Goodwin, "Profiles of HCO and CH_3 in CH_4/O_2 and C_2H_4/O_2 Flames by Resonance Ionization," in *Twenty-Second Symposium (International) on Combustion* (Combustion Institute, Pittsburgh, PA, 1988), p. 1421.
16. J. S. Bernstein, X.-M. Song, and T. A. Cool, "Detection of the Formyl Radical in a Methane/Oxygen Flame by Resonance Ionization," Chem. Phys. Lett. **145,** 188–192 (1988).
17. W. G. Mallard, J. H. Miller, and K. C. Smyth, "The ns Rydberg Series of 1,3-*trans*-Butadiene Observed Using Multiphoton Ionization," J. Chem. Phys. **79,** 5900–5905 (1983); see also P. H. Taylor, W. G. Mallard, and K. C. Smyth, "Multiphoton Ionization Spectra of *trans*-1,3-Butadiene: Reassignment of a Rydberg Series," J. Chem. Phys. **84,** 1053–1055 (1986).
18. K. C. Smyth, J. H. Miller, R. C. Dorfman, W. G. Mallard, and R. J. Santoro, "Soot Inception in a Methane/Air Diffusion Flame as Characterized by Detailed Species Profiles," Combust. Flame **62,** 157–181 (1985).
19. J. H. Miller and P. H. Taylor, "Methyl Radical Concentrations and Production Rates in a Laminar Methane/Air Diffusion Flame," Combust. Sci. Technol. **52,** 139–149 (1987).
20. K. C. Smyth, P. J. H. Tjossem, A. Hamins, and J. H. Miller, "Concentration Measurements of OH· and Equilibrium Analysis in a Laminar Methane-Air Diffusion Flame," Combust. Flame **79,** 366–380 (1990).
21. J. H. Miller, W. G. Mallard, and K. C. Smyth, "Chemical Production Rates of Intermediate Hydrocarbons in a Methane/Air Diffusion Flame," in *Twenty-First Symposium (International) on Combustion* (Combustion Institute, Pittsburgh, PA, 1986), p. 1057.
22. K. C. Smyth and J. H. Miller, "Chemistry of Molecular Growth Processes in Flames," Science **236,** 1540–1546 (1987).
23. H. F. Calcote, "Mechanisms of Soot Nucleation in Flames—A Critical Review," Combust. Flame **42,** 215–242 (1981).
24. H. F. Calcote, D. B. Olson, and D. G. Keil, "Are Ions Important in Soot Formation?," Energy Fuels **2,** 494–504 (1988).
25. G. J. Havrilla, P. K. Schenck, J. C. Travis, and G. C. Turk, "Signal Detection of Pulsed Laser-Enhanced Ionization," Anal. Chem. **56,** 186–193 (1984).
26. T. A. Cool, "Quantitative Measurement of NO Density by Resonance Three-Photon Ionization," Appl. Opt. **23,** 1559–1572 (1984).
27. R. E. Imhof, F. H. Read, and S. T. Beckett, "Determination of the Transition Moment of the $B^1\Sigma^+$—$X^1\Sigma^+$ Transition in CO," J. Phys. B **5,** 896–902 (1972).
28. Certain commercial equipment is identified herein to specify the experimental procedures. Such identification does not imply recommendation by the National Institute of Standards and Technology, nor does it imply that this equipment is the best available for the purpose.
29. A. Hamins and J. H. Miller, (1989); unpublished results.
30. L. Li, M. Wu, and P. M. Johnson, "One- and Two-Color Multiphoton Ionization of Argon," J. Chem. Phys. **89,** 3470–3478 (1988).
31. J. H. Miller, W. G. Mallard, and K. C. Smyth, "The Observation of Laser-Induced Visible Fluorescence in Sooting Diffusion Flames," Combust. Flame **47,** 205–214 (1982).
32. F. Beretta, V. Cincotti, A. D'Alessio, and P. Menna, "Ultraviolet and Visible Fluorescence in the Fuel Pyrolysis Regions of Gaseous Diffusion Flames," Combust. Flame **61,** 211–218 (1985).
33. A. Savitzky and M. J. E. Golay, "Smoothing and Differentiation of Data by Simplified Least Squares Procedures," Anal. Chem. **36,** 1627–1639 (1964).
34. M.-S. Chou, A. M. Dean, and D. Stern, "Laser-Induced Fluorescence and Absorption Measurements of NO in NH_3/O_2 and CH_4/Air Flames," J. Chem. Phys. **78,** 5962–5970 (1983).
35. J. Brzozowski, N. Elander, and P. Erman, "Direct Measurements of Lifetimes of Low-Lying Excited Electronic States in Nitric Oxide," Phys. Scr. **9,** 99–103 (1974).
36. S. T. Pratt, P. M. Dehmer, and J. L. Dehmer, "Photoelectron Studies of Resonant Multiphoton Ionization of Molecular Nitrogen," J. Chem. Phys. **81,** 3444–3451 (1984).
37. J. E. M. Goldsmith, "Photochemical Effects in 205-nm, Two-Photon-Excited Fluorescence Detection of Atomic Hydrogen in Flames," Opt. Lett. **11,** 416–418 (1986).
38. J. E. M. Goldsmith, "Photochemical Effects in 243-nm, Two-Photon Excitation of Atomic Hydrogen in Flames," Appl. Opt. **28,** 1206–1213 (1989).
39. W. G. Mallard and K. C. Smyth, "Mobility Measurements of Atomic Ions in Flames Using Laser-Enhanced Ionization," Combust. Flame **44,** 61–70 (1982).